PREPARED FOR THE U.S. DEPARTMENT OF ENERGY,
UNDER CONTRACT DE-AC02-76CH03073

PPPL-3799
UC-70

PPPL-3799

Flux Rope Acceleration and Enhanced Magnetic Reconnection Rate

by

C.Z. Cheng, Y. Ren, G.S. Choe, and Y.-J. Moon

March 2003

PPPL
PRINCETON PLASMA PHYSICS LABORATORY

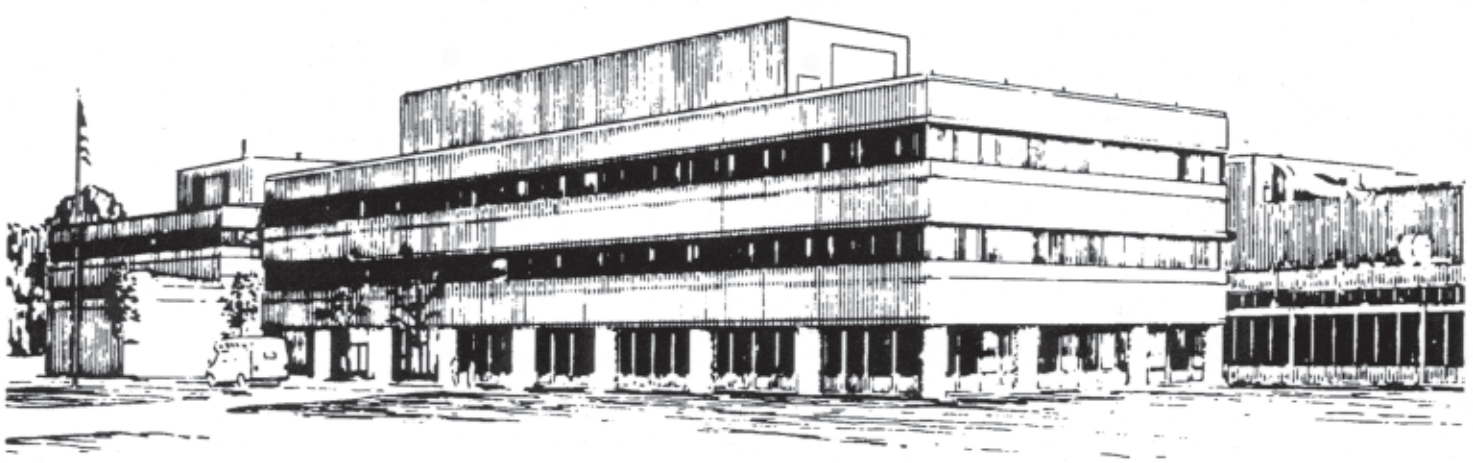

PRINCETON PLASMA PHYSICS LABORATORY
PRINCETON UNIVERSITY, PRINCETON, NEW JERSEY

PPPL Reports Disclaimer

Availability

This report is posted on the U.S. Department of Energy's Princeton Plasma Physics Laboratory Publications and Reports web site in Fiscal Year 2003. The home page for PPPL Reports and Publications is: http://www.pppl.gov/pub_report/

DOE and DOE Contractors can obtain copies of this report from:

U.S. Department of Energy
Office of Scientific and Technical Information
DOE Technical Information Services (DTIS)
P.O. Box 62
Oak Ridge, TN 37831

Telephone: (865) 576-8401

Fax: (865) 576-5728

Email: reports@adonis.osti.gov

This report is available to the general public from:

National Technical Information Service
U.S. Department of Commerce
5285 Port Royal Road
Springfield, VA 22161

Telephone: 1-800-553-6847 or
(703) 605-6000

Fax: (703) 321-8547

Internet: http://www.ntis.gov/ordering.htm

Submitted to Ap.J.

FLUX ROPE ACCELERATION AND ENHANCED MAGNETIC RECONNECTION RATE

C. Z. CHENG[1], Y. REN[1], G. S. CHOE[1], AND Y.-J. MOON[2,3]

ABSTRACT

A physical mechanism of flares, in particular for the flare rise phase, has emerged from our 2-1/2D resistive MHD simulations. The dynamical evolution of current sheet formation and magnetic reconnection and flux rope acceleration subject to continuous, slow increase of magnetic shear in the arcade are studied by employing a non-uniform anomalous resistivity in the reconnecting current sheet under gravity. The simulation results directly relate the flux rope's accelerated rising motion with an enhanced magnetic reconnection rate and thus an enhanced reconnection electric field in the current sheet during the flare rise phase. The simulation results provide good quantitative agreements with observations of the acceleration of flux rope, which manifests in the form of SXR ejecta or erupting filament or CMEs, in the low corona. Moreover, for the X-class flare events studied in this paper the peak reconnection electric field is $\sim O(10^2\,\mathrm{V/m})$ or larger, enough to accelerate particles to over 100 keV in a field-aligned distance of 10 km. Nonthermal electrons thus generated can produce hard X-rays, consistent with impulsive HXR emission observed during the flare rise phase.

Subject headings: Sun: flares—Sun: coronal mass ejections (CMEs)—MHD—methods: numerical

1. Introduction

Solar flares are intense, abrupt release of energy occurring usually in a solar active region. In the last decade the Hard X-Ray Telescope (HXT) and Soft X-Ray Telescope (SXT) on

[1]Princeton Plasma Physics Laboratory, Princeton University, Princeton, NJ 08543-0451 (fcheng@pppl.gov)

[2]Big Bear Solar Observatory, NJIT, 40386 North Shore Lane, Big Bear City, CA 92314

[3]Korea Astronomy Observatory, Whaam-dong, Yuseong-gu, Daejeon 305-348, Korea

board the Japanese Yohkoh satellite have revealed many important flare processes. Tsuneta et al. (1992) found that long duration event type flares observed in the solar limb often have cusp-like soft X-ray (SXR) loops. The height and the footpoint separation of the SXR loops increase as a function of time, and the outer loops have a higher temperature. Masuda et al. (1994) found that in impulsive flares a hard X-ray (HXR) source is located above the SXR loop. The region around the loop-top HXR source has higher temperature than in the SXR flare loop. Impulsive flares also have an HXR double-source structure at the footpoints and the separation of the two sources increases with time in most flares. These observations clearly support the classical "CSHKP" (Carmichael-Sturrock-Hirayama-Kopp-Pneuman) model of magnetic reconnection (Sturrock 1992) with the location of a reconnection site above the top of the SXR loops in the low corona. Particles are accelerated to high energy ($> 10\,\mathrm{keV}$) by the reconnection electric field in the reconnecting current sheet region. The loop top HXR source results from the bremsstrahlung emission of nonthermal electrons ($> 10\,\mathrm{keV}$). The two-ribbon structure of HXR emission forms when nonthermal electrons follow the newly reconnected field lines and hit the dense and cold chromosphere to emit hard X-rays by bremsstrahlung.

The magnetic reconnection model of flares is further supported by the recent observation of a long duration X5.7 class flare event in the solar disk on July 14, 2000 (called the Bastille day event). For the Bastille day event TRACE (Transition Region And Coronal Explorer) observed an arcade structure in the EUV wavelength range with the width and length being $\sim 30,000\,\mathrm{km}$ and $180,000\,\mathrm{km}$, respectively, and the Yohkoh HXT observed for the first time a two-ribbon structure in the chromosphere in HXR emission with energy above $30\,\mathrm{keV}$ during the flare's impulsive phase (Masuda et al. 2001). The HXR spectrum is harder at the outer edge (corresponding to newly reconnected field lines) of the ribbons than at the inner edge (corresponding to field lines reconnected earlier). The results indicate that nonthermal electrons move to the chromosphere from the acceleration site in the magnetic reconnection region, which is above the SXR loop, along the whole length of the arcade, not merely in a particular dominant loop.

Most arcade reconnection models of flares predict a plasmoid, which is a flux rope with helical field lines in 2-1/2D or a helical magnetic structure loosely connected to the solar surface in 3D, is formed above the reconnection current sheet by reconnection of line-tied field lines. The flux rope is identified in the Yohkoh observations as an SXR plasma ejecta which is frequently observed above the SXR loops (Hudson 1994; Shibata et al. 1995; Ohyama & Shibata 1997, 1998). Some SXR plasma ejecta were launched well before the flare impulsive phase. In particular, the SXR plasma ejecta have two phases of rising motion: the first phase with slow rising speed coincides with the preflare phase, and the second phase with accelerated rising speed coincides with the flare impulsive phase with the HXR emission

impulsively enhanced. Thus, the Yohkoh observations establish a correlation between the flare energy release and SXR plasma ejecta upward motion.

Observations have also revealed that a significant percentage ($> 50\%$) of coronal mass ejections (CMEs) are accompanied by X-ray flares (Munro et al. 1979; Sheeley, Jr. et al. 1983; Webb & Hundhausen 1987; St. Cyr & Webb 1991; Harrison 1995). The apparent association between CMEs and X-ray flares suggest that there is a common physical mechanism underlying both phenomena (Kahler 1992; Gosling 1993; Dryer 1994; Hundhausen 1999). Recently, the cause-effect relationship between CME propagation and X-ray flare emission has been actively examined based on the combined observations of SOHO LASCO, SOHO MDI, SOHO EIT, BBSO H_α, TRACE, GOES, Yohkoh SXT and HXT, and the Ramaty High Energy Solar Spectroscopic Imager (RHESSI) (Alexander et al. 2001; Neupert et al. 2001; Zhang et al. 2001; Moon et al. 2002; Yurchyshyn 2002; Gallaghar et al. 2003). In particular, Moon et al. (2002) have studied the cause-effect relationship between CME propagation and X-ray flare emission for a set of homologous flares and their associated CME motion, and found that CMEs are accelerated in the low corona during the flare rise phase. Figure 1 shows the correlation of the CME acceleration in the low corona in the form of filament eruption with the rise phase of the 2000 November 24 X1.8 X-ray flare (Moon et al. 2002). An impulsive hard X-ray emission was also observed around 21:52UT during the flare rise phase. Similarly, a rapid acceleration of a CME in the low corona is found to be associated with the rise phase of the 2002 April 21 X1.5 flare (Gallaghar et al. 2003). The event is first observed as a rapid rise in GOES X-rays, followed by simultaneous conjugate footpoint brightening connected by an ascending flux rope feature. The most intense peak in hard X-rays ($\geq 25\,\mathrm{keV}$) observed by RHESSI (Gallaghar et al. 2002) occurs at the time of maximum acceleration of the CME upward motion. It is thus quite convincing that the CME-flare observations have established a correlation between the flare energy release and CME upward motion.

From these observations we note that the association of impulsive CME acceleration in the low corona with the flare rise phase is similar to the the association of impulsive SXR ejecta acceleration with the impulsive hard X-ray emission (Ohyama & Shibata 1997). Based on the magnetic reconnection model, both the CME and SXR plasma ejecta motions in the low corona can be considered as the motion of a flux rope. Thus, these different physical phenomena reduce essentially to a common fundamental physical mechanism that the impulsive flux rope acceleration is associated with the flare rise phase and the impulsive hard X-ray emission. It is thus the objective of this paper to examine the physical mechanism of the flare X-ray emission and flux rope upward motion.

Although the flare morphology supports the CSHKP-like field configuration in the vicin-

ity of and under the reconnection site, the observation of flux rope acceleration and associated reconnection rate cannot be interpreted within the scope of the CSHKP model. The possibility of flux rope formation and its rising motion has indeed been confirmed by several 2D and 2-1/2D numerical simulations (Mikic et al. 1988; Forbes 1990, 1991; Inhester et al. 1992; Mikic & Linker 1994; Linker & Mikic 1995; Kusano et al. 1995; Choe & Lee 1996; Amari et al. 1996; Magara et al. 1996; Choe & Cheng 2000; Chen & Shibata 2000; Cheng & Choe 2001), but the correlation between the flux rope motion and reconnection rate has not been studied systematically. In the CSHKP model, the rise of the flux rope can be considered as a process of approaching a new equilibrium state after a change in field topology. Thus, the flux rope rising motion must eventually decelerate unless the reconnection of arcade field lines under the flux rope continues indefinitely.

To understand the observations of impulsive flux rope acceleration in the low corona, which can occur in the form of filament eruption or X-ray plasma ejection or CME, and its correlation with the enhanced flare X-ray emission, we present a flare model in terms of the dynamical evolution of flux rope motion and magnetic reconnection rate. Our flare model is based on 2-1/2D resistive MHD simulations, and we found that the magnetic reconnection rate in the current sheet is enhanced when the flux rope upward motion is impulsively accelerated in the low corona. The acceleration of flux rope can be further enhanced if it merges with a pre-existing upper flux rope. The reconnection electric field, which can reach $\sim O(10^2)\,\mathrm{V/m}$, is essentially directed along the ambient magnetic field in the reconnecting current sheet, and can easily accelerate electrons to a hard X-ray emitting energy of 100 keV in a distance of $> 1\,\mathrm{km}$ along the ambient magnetic field to produce the impulsive hard X-ray emission during the flare rise phase. It should be emphasized that our simulation results are the first to provide an explanation for the observed correlation between the flux rope acceleration and enhanced magnetic reconnection rate.

2. Flux Rope Acceleration and Enhanced Reconnection Rate

Our model for understanding the observations of impulsive flux rope acceleration in the low corona and its correlation with the enhanced flare X-ray emission is based on resistive 2-1/2D MHD simulations of the evolution of a bipolar arcade (Choe & Cheng 2000; Cheng & Choe 2001). The evolution of our model corona is governed by resistive MHD equations including gravity and resistivity and assuming the plasma to be isothermal. The magnetic field $\mathbf{B}$ is normalized by B_0 which is the maximum magnitude of the initial boundary normal field, the mass density ρ is normalized by the initial density ρ_0 at the bottom boundary, the velocity $\mathbf{v}$ is normalized by $v_0 = B_0/(4\pi\rho_0)^{1/2}$, the time t is normalized by $t_0 = L_0/v_0$, and

the resistivity η is normalized by $L_0 v_0$, where L_0 is the length unit. A non-uniform grid is employed to resolve the current sheet structure.

We consider the evolution of an initially closed arcade field configuration in the (x,y) plane and the magnetic field is invariant in the z-direction. The gravity is pointing downward in the y-coordinate. The magnetic field can be expressed as $\mathbf{B} = \nabla\psi(x,y,t) \times \nabla z + B_z(x,y,t)\nabla z$, where ψ is the poloidal magnetic flux. A non-uniform anomalous resistivity model (e.g., Ugai 1985; Scholer & Roth 1987; Yan et al. 1992; Yokoyama & Shibata 1994; Choe & Lee 1996; Schumacher & Kliem 1996; Ugai 1999) is employed with $\eta = \eta_0(j_z/j_c - 1)^2$ for $j_z > j_c$ and $\eta = 0$ for $j_z \leq j_c$, $\eta_0 = 10^{-5}$, $j_c = 1.5$. We focus on the evolution of flux ropes not totally expelled from the sun. By imposing a shear-increasing footpoint motion with a shearing velocity $V_z(x) = V_{z0}\, x\, \exp[(1-x^2)/2]$ and $V_{z0} = 10^{-3} v_0$, magnetic reconnection takes place to create flux ropes, and merging of flux ropes also occur in the corona as shown in Fig. 2, which shows the flux rope's O-line height versus time. There are four reconnection events in the simulation, and the cross sign in the figure indicates the formation of a new flux rope and the circle sign indicates the completion of the merging of two flux ropes. It is clear that each reconnection event occurs in a very short time scale. We note that in the first reconnection event there is no flux rope merging involved.

As the X-line and the current sheet below the newborn flux rope rise, the field structure in the current sheet changes rapidly. When a flux rope is formed, the toroidal flux originally contained in the line-tied flux arcade is redistributed into two flux systems: the flux rope and the underlying line-tied arcade field. The magnetic shear is thus reduced in the underlying arcade after flux rope formation. A further increase of the magnetic shear takes place in the lower arcade flux system, and above a critical value of magnetic shear magnetic reconnection causes a new flux rope to form as shown in Fig. 3, which shows the 3D field lines of flux ropes and closed arcade fields as well as their projection in the (x,y) plane. We note that in the flux ropes the toroidal field (B_z) is larger than the poloidal field ($B_p = |\nabla\psi|$). In the current sheet below the newborn flux rope, $B_z \gg B_p$ and the field line is almost along the neutral line direction (the z-direction). But, in the arcade below the current sheet, $B_z \sim B_p$. When magnetic reconnection continues, the newborn flux rope rises with an accelerated velocity and eventually merges with the overlying flux rope to form a single integrated flux rope. This process of new flux rope formation and its merging with a pre-existing flux rope can be repeated as long as the magnetic shear is continuously supplied.

Figure 4 shows the detailed time evolution of the flux rope's O-line height, velocity, acceleration (a) and magnetic reconnection rate ($\partial\psi/\partial t$, where ψ is the magnetic flux at the X-line) for the four magnetic reconnection events shown in Figure 2. From the Faraday's law the reconnection electric field at the X-line is related to the magnetic reconnection rate by

$E_z = -\partial\psi/\partial t$ in our 2-1/2D model. We note that for the first three reconnection events the flux rope is first accelerated and then decelerated, while for the fourth reconnection event after the first acceleration the flux rope's velocity saturates and then it is re-accelerated and then decelerated again. From Figure 4 we see that the reconnection rate increases during the flux rope first acceleration phase and then gradually decreases for a longer duration after the first flux rope acceleration subsides for all these four reconnection events. The acceleration of the newborn flux rope's rising motion is similar to the accelerated motion of soft X-ray ejecta in the flare impulsive phase observed by Yohkoh (Ohyama & Shibata 1997, 1998) and the accelerated CME motion in the rise phase of X-ray flares (Moon et al. 2002; Gallaghar et al. 2003). We also note that the flux rope acceleration and reconnection rate are further enhanced when the magnetic merging process occurs. The reconnection electric field is peaked in the current sheet below the newborn flux rope. Moreover, because the reconnection electric field is mainly parallel to the magnetic field in the current sheet, particles can be accelerated to very high energy along the field line if the reconnection electric field is large. If we assume that the flare X-ray emission is proportional to the magnetic reconnection rate, our simulation results of flux rope acceleration and associated enhanced reconnection rate resemble the observations of flux rope acceleration in the low corona and its association with the flare rise phase and impulsive hard X-ray emission (Ohyama & Shibata 1997, 1998; Moon et al. 2002; Gallaghar et al. 2003).

From the simulation results, the phase of the newborn flux rope creation and its slow rise is regarded as the preflare phase, the accelerated newborn flux rope rise phase is interpreted as the impulsive phase, and the phase with a longer period of weaker reconnection rate is considered as the main phase of a flare. The sequence of the above flaring events (reconnection processes) can be repeated as long as the magnetic shear is replenished, and we propose that they constitute a set of homologous flares.

3. Comparisons with Observations

Now, we make quantitative comparisons of the modeling results with observations during the X-ray flare rise phase. We first compare the third model reconnection event shown in Figure 4 with the flare-CME observations shown in Figure 1 for the 2000 November 24 X1.8 X-ray flare (Moon et al. 2002). We consider a two million degree coronal background plasma, and choose the maximum magnitude of the lower corona boundary normal field to be $B_0 = 300\,\mathrm{G}$, the lower boundary electron density to be $n_0 = 10^9\,\mathrm{cm}^{-3}$, and the length scale normalization $L_0 = 6 \times 10^4\,\mathrm{km}$. Then, the distance between the opposite main magnetic patches in the corona base is $2L_0 = 1.2 \times 10^5\,\mathrm{km}$, the velocity normalization

is $V_0 = B_0/(4\pi m_p n_0)^{1/2} = 2 \times 10^4\,\mathrm{km/s}$, the time scale normalization is $t_0 = L_0/V_0 = 3\,\mathrm{s}$, the acceleration normalization is $a_0 = V_0/t_0 = 6.7 \times 10^3\,\mathrm{km/s^2}$, and the electric field normalization is $E_0 = V_0 B_0/c = 6 \times 10^5\,\mathrm{V/m}$. From the third reconnection event shown in Figure 4, we obtain the maximum acceleration of $a_{max} \simeq 4.3\,\mathrm{km/s^2}$ at the flux rope height of $\simeq 2.4 \times 10^5\,\mathrm{km}$, and the maximum velocity reaches $V_{max} \simeq 2200\,\mathrm{km/s}$ the flux rope height of $\simeq 10^6\,\mathrm{km}$. The maximum velocity is reached in a flux rope acceleration period of about 15 min, which compares well with the active acceleration period of about 15 min between 21:45 and 22:00 UT shown in Fig. 1. For the 2000 November 24 X1.8 X-ray flare event, the distance between the opposite main magnetic patches in the active region is about $1.1 \times 10^5\,\mathrm{km}$ (Moon et al. 2002). From Figure 1 the acceleration reaches a maximum value of $a_{max} \simeq 4.5\,\mathrm{km/s^2}$ at the height of $\simeq 2.2 \times 10^5\,\mathrm{km}$, and the maximum velocity $V_{max} \simeq 2300\,\mathrm{km/s}$ is reached at the height of $\simeq 1.1 \times 10^6\,\mathrm{km}$. The maximum velocity is reached in a flux rope acceleration period of about 15 min. Therefore, the modeling numbers agree quite well with the observation. Moreover, at the time of maximum reconnection rate the reconnection electric field is $E_{zmax} \simeq 1000\,\mathrm{V/m}$, which is much larger than the Dreicer electric field of $\approx 10^{-2}\,\mathrm{V/m}$ for coronal parameters of a background proton number density of $n_p = 10^{10}\,\mathrm{cm^{-3}}$ and an electron temperature of $T_e = 1\,\mathrm{keV}$. Thus, the collisional drag force to the electron motion in the acceleration region can be neglected. With this magnetic field-aligned electric field electrons can be accelerated to $\simeq 10^3\,\mathrm{keV}$ in a field-aligned distance of $\geq 1\,\mathrm{km}$ in the current sheet.

Next, we compare the first model reconnection event shown in Figure 4 with the Yohkoh observation of the 1993 November 11 C9.7 flare that showed an accelerated SXR ejecta motion and associated impulsive HXR emission as shown in Figure 3 of Ohyama & Shibata (1997). For this flare event the SXR ejecta rises to a height of $\simeq 2.6 \times 10^4\,\mathrm{km}$ with a velocity of $\simeq 60\,\mathrm{km/s}$ at 11:16UT, rises to $\simeq 3 \times 10^4\,\mathrm{km}$ with a velocity of $\simeq 110\,\mathrm{km/s}$ at 11:17UT, to $\simeq 3.8 \times 10^4\,\mathrm{km}$ with a velocity of $\simeq 140\,\mathrm{km/s}$ at 11:18UT, to $\simeq 4.9 \times 10^4\,\mathrm{km}$ with a velocity of $\simeq 160\,\mathrm{km/s}$ at 11:19UT, to $\simeq 5.8 \times 10^4\,\mathrm{km}$ with a velocity of $\simeq 180\,\mathrm{km/s}$ at 11:20UT, and then rises almost linearly to $\simeq 9 \times 10^4\,\mathrm{km}$ with a velocity of $\simeq 200\,\mathrm{km/s}$ at 11:23UT. Thus, there is a SXR ejecta acceleration phase during 11:16 - 11:23UT. The maximum acceleration occurs at about 11:17:30UT. Note that HXR emission in the 14-23 keV HXT energy band is enhanced during 11:15 - 11:26UT and for the 23-33 keV HXT energy band it is enhanced during 11:15 - 11:18UT. To compare the first reconnection event shown in Figure 4 with this Yohkoh event, we choose the maximum normal magnetic field at the corona base to be $B_0 = 200\,\mathrm{G}$, the lower boundary electron density to be $n_0 = 10^9\,\mathrm{cm^{-3}}$, and the length scale normalization to be $L_0 = 2.2 \times 10^4\,\mathrm{km}$. Then, the distance between the opposite main magnetic patches in the corona base is $2L_0 = 4.4 \times 10^4\,\mathrm{km}$, the velocity normalization is $V_0 = B_0/(4\pi m_p n_0)^{1/2} = 1.3 \times 10^4\,\mathrm{km/s}$, the time scale normalization is

$t_0 = L_0/V_0 = 1.7\,\mathrm{s}$, the acceleration normalization $a_0 = V_0/t_0 = 7.6 \times 10^3\,\mathrm{km/s^2}$, and the electric field normalization is $E_0 = V_0 B_0/c = 2.6 \times 10^4\,\mathrm{V/m}$. For the first model reconnection event shown in Figure 4, if we assume that the flux rope begins to be accelerated at 11:16UT, then the maximum velocity reaches $V_{max} \simeq 210\,\mathrm{km/s}$ at the flux rope height of $8.4 \times 10^4\,\mathrm{km}$ at about 11:23UT. The maximum acceleration $a_{max} \simeq 0.73\,\mathrm{km/s^2}$ occurs at the flux rope height of $5 \times 10^4\,\mathrm{km}$ at about 11:20UT. At the maximum reconnection rate the maximum reconnection electric field is $E_{zmax} \simeq 23\,\mathrm{V/m}$ at about 11:26UT. These model numbers are in reasonably good agreement with the observations shown in Figure 3 of Ohyama & Shibata (1997).

These two encouraging quantitative comparisons between our modeling results and observations strongly suggest that the magnetic reconnection model is responsible for the observed flux rope acceleration and flare rise phase because the reconnection rate is impulsively enhanced during the flux rope acceleration and the enhanced reconnection electric field is large enough to accelerate particles to high energies. On the other hand, we emphasize that the simulated flux rope motion is compared with observations only in the low corona because our simulations address only the flare mechanism and not the escape of flux rope from the sun as in the CME observation. In our simulation, the flux rope speed decreases as the reconnection rate decreases. The issue of flux rope escape would require the flux rope to break through the overlying fields possibly by the expansion of the overlying fields and continuing magnetic reconnection below the flux rope, which is beyond the scope of the present study.

4. Summary and Discussion

A physical mechanism of flares, in particular for the flare rise phase, has emerged from our 2-1/2D MHD simulations with nonuniform anomalous resistivity. The simulation results are very encouraging because they directly relate the flux rope's accelerated rising motion with an enhanced magnetic reconnection rate and thus an enhanced reconnection electric field in the current sheet during the flare rise phase. Moreover, the peak reconnection electric field is $\sim O(10^2\,\mathrm{V/m})$ or larger, enough to accelerate particles to over 100 keV in a field-aligned distance of 10 km. Nonthermal electrons thus generated can produce hard X-rays, consistent with impulsive HXR emission observed during the flare rise phase. It should be emphasized that our simulation results are the first to provide a good agreement with observations of the acceleration of flux rope, which manifests in the form of SXR ejecta or erupting filament or CMEs, in the low corona during the flare rise phase.

Several important issues must still be addressed in the proposed magnetic reconnection model for the dynamics of flux rope and current sheet during the flare rise phase. First

of all, how current sheet configurations are formed dynamically and how fast reconnection occurs. In our MHD simulation model we supply magnetic shear in the coronal arcade field by the photospheric shear-increasing footpoint motion and above a critical magnetic shear, current sheet is formed to allow magnetic reconnection to occur. Observations also support the emergence of pre-sheared magnetic flux through the chromosphere into the corona (e.g., Kundu et al. 1989; Kurokawa 1989). MHD simulations have also shown that buoyant emerging flux can create a current sheet by interacting with the existing coronal magnetic field (Yokoyama & Shibata 1996). Thus, it is important to study the effect of magnetic shear increasing process on current sheet formation and fast reconnection by considering more general footpoint motion as well as the emergence of pre-sheared magnetic flux. Moreover, we need to improve our simulation model to 3D geometries with a spherical boundary as in the real sun. In particular, the geometry of the current sheet and magnetic reconnection process in a 3D geometry can be significantly different from the 2-1/2D case, and 3D simulations can provide a much more realistic assessment of the flux rope structure and how flux rope motion is related to the flare energy release.

This work was supported by the DoE Contract No. DE-AC02-76-CHO3073. Y.-J. M. is supported by a MURI grant of AFOSR and by National Research Lab. M10104000059-01J000002500 of the Korean government.

REFERENCES

Alexander, D., Metcalf, T. R., & Nitta, N. 2001, Geophys. Res. Lett., 29, 13670

Amari, T., Luciani, J. F., Aly, J. J., & Tagger, M. 1996, A&A, 306, 913

Chen, P. F. & Shibata, K. 2000, ApJ, 545, 524

Cheng, C. Z. & Choe, G. S. 2001, Earth, Planets and Space, 53, 597

Choe, G. S. & Cheng, C. Z. 2000, ApJ, 541, 449

Choe, G. S. & Lee, L. C. 1996, ApJ, 472, 372

Dryer, M. 1994, Space Sci. Rev., 67, 363

Forbes, T. G. 1990, J. Geophys. Res., 95, 11919

—. 1991, Geophys. Astrophys. Fluid Dyn., 62, 15

Gallaghar, P. T., Dennis, B. R., Krucker, S., Schwartz, R. A., & Tolbert, A. K. 2002, Sol. Phys., 210, to appear

Gallaghar, P. T., Lawrence, G. R., & Dennis, B. R. 2003, ApJ, to be submitted

Gosling, J. T. 1993, J. Geophys. Res., 98, 18937

Harrison, R. A. 1995, A&A, 304, 585

Hudson, H. S. 1994, in Proceedings of Kofu Symposium, 1

Hundhausen, A. J. 1999, in The Many Faces of the Sun, ed. K. T. Strong, J. L. R. Saba, B. M. Haisch, & J. T. Schmelz (New York: Springer-Verlag), 143

Inhester, B., Birn, J., & Hesse, M. 1992, Sol. Phys., 138, 257

Kahler, S. W. 1992, ARA&A, 30, 113

Kundu, M., Woodgate, B. E., & Schmahl, E. J., eds. 1989, Energetic Phenomena on the Sun (Kluwer Academic Publishers, Dordrecht)

Kurokawa, H. 1989, Space Sci. Rev., 51, 49

Kusano, K., Suzuki, Y., & Nishikawa, K. 1995, ApJ, 441, 942

Linker, J. A. & Mikic, Z. 1995, ApJ, 438, L45

Magara, T., Mineshige, S., Yokoyama, T., & Shibata, K. 1996, ApJ, 466, 1054

Masuda, S., Kosugi, T., Hara, H., Tsuneta, S., & Ogawara, Y. 1994, Nature, 371, 495

Masuda, S., Kosugi, T., & Hudson, H. S. 2001, Sol. Phys., 204, 57

Mikic, Z., Barnes, D. C., & Schnack, D. D. 1988, ApJ, 328, 830

Mikic, Z. & Linker, J. A. 1994, ApJ, 430, 898

Moon, Y.-J., Moon, Y. J., Choe, G. S., Wang, H., Park, Y. D., & Cheng, C. Z. 2002, ApJ, submitted

Munro, R. H., Gosling, J. T., MacQueen, E. H. R. M., Poland, A. I., & Ross, C. L. 1979, Sol. Phys., 61, 201

Neupert, W. M., Thompson, B. J., Gurman, J. B., & Plunkett, S. P. 2001, J. Geophys. Res., 106, 25215

Ohyama, M. & Shibata, K. 1997, PASJ, 49, 249

—. 1998, ApJ, 499, 934

Scholer, M. & Roth, D. 1987, J. Geophys. Res., 2, 3223

Schumacher, J. & Kliem, B. 1996, Phys. Plasmas, 3, 4703

Sheeley, Jr., N. R., Howard, R. A., Koomen, M. J., & Michels, D. J. 1983, ApJ, 272, 349

Shibata, K., Masuda, S., Hara, H., Yokoyama, T., Tsuneta, S., Kosugi, T., & Ogwara, Y. 1995, ApJ, 451, L83

St. Cyr, O. C. & Webb, D. F. 1991, Sol. Phys., 136, 379

Sturrock, P. A. 1992, in Eruptive Solar Flares, IAU Colloquium 133, Lecture Notes in Physics, 399, ed. Z. Švestka, B. V. Jackson, & M. E. Machado (Berlin: Springer-Verlag), 397

Tsuneta, S., Hara, H., Shimizu, T., Acton, L. A., Strong, K. T., Hudson, H. S., & Ogawara, Y. 1992, PASJ, 44, L63

Ugai, M. 1985, Plasma Phys. Controlled Fusion, 27, 1183

—. 1999, J. Geophys. Res., 104, 6929

Webb, D. F. & Hundhausen, A. J. 1987, Sol. Phys., 108, 383

Yan, M., Lee, L. C., & Priest, E. R. 1992, J. Geophys. Res., 97, 8277

Yokoyama, T. & Shibata, K. 1994, ApJ, 436, L197

—. 1996, PASJ, 48, 353

Yurchyshyn, V. B. 2002, ApJ, 576, 493

Zhang, J., Dere, K. P., Howard, R. A., Kundu, M. R., & White, S. M. 2001, ApJ, 559, 452

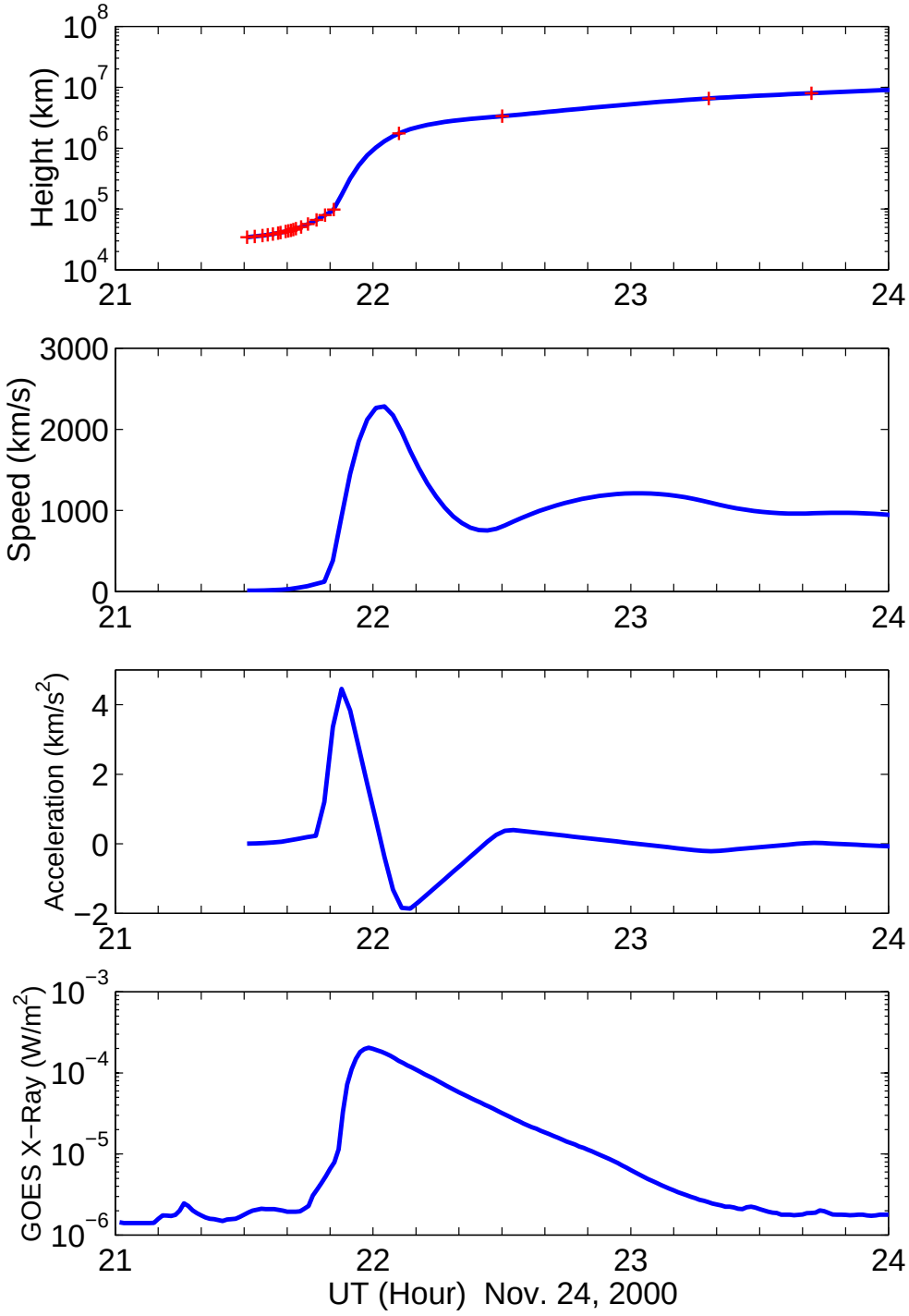

Fig. 1.— The time evolution of height (relative to the solar limb), speed and acceleration of the filament eruption in the low corona and CME in the higher corona associated with a 2000 November 24 X1.8 flare and the corresponding GOES X-ray flux. The impulsive HXR emission occurs around 21:52 UT which coincides with the peak CME acceleration.

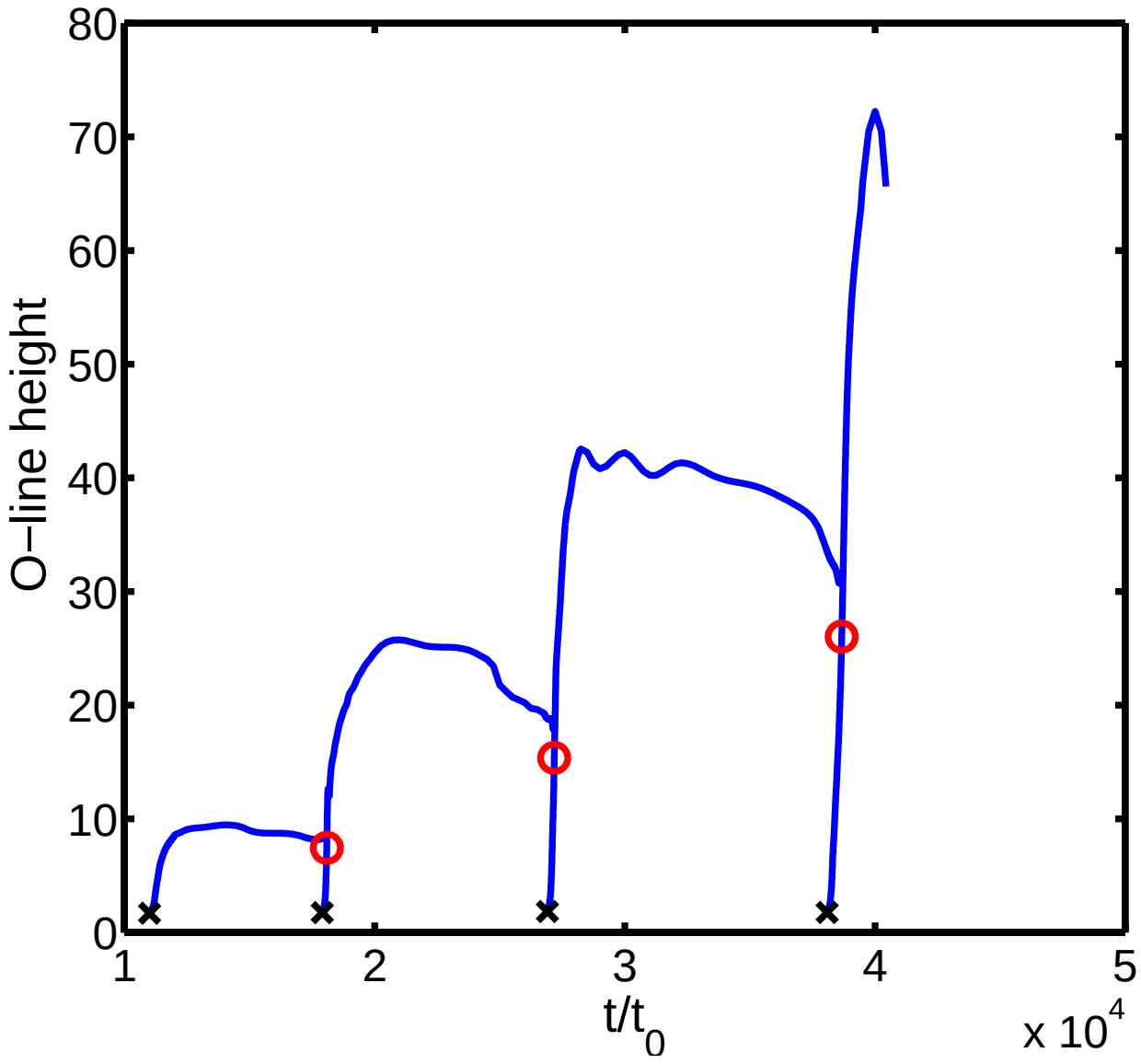

Fig. 2.— The height of O-lines of the flux ropes versus time for the MHD simulation with a non-uniform anomalous resistivity model with the resistivity parameters $\eta_0 = 10^{-5}$, $j_c = 1.5$, and the photospheric velocity shear parameter $V_{z0} = 10^{-3}\, V_0$. The slope of the curves represents the rising speed of the flux ropes. The cross sign indicates the formation of a new flux rope and the circle sign indicates the completion of the merging of two flux ropes.

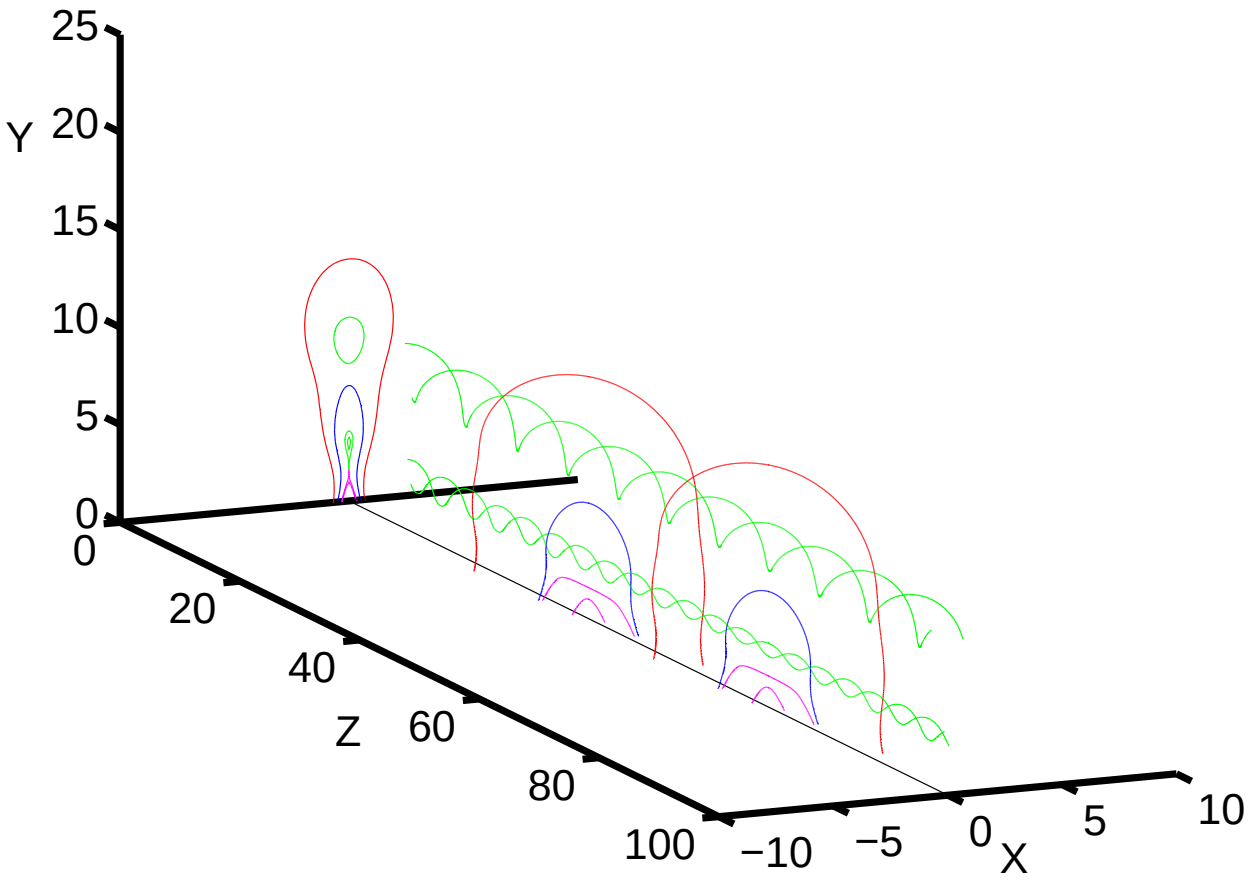

Fig. 3.— 3D magnetic field lines and their projection in the (x,y) plane at $t = 18020\,t_0$ in a 2-1/2D MHD simulation with the maximum shearing velocity $V_{z0} = 10^{-3}\,V_0$ and the non-uniform resistivity parameters $\eta_0 = 10^{-5}$, and $j_c = 1.5$.

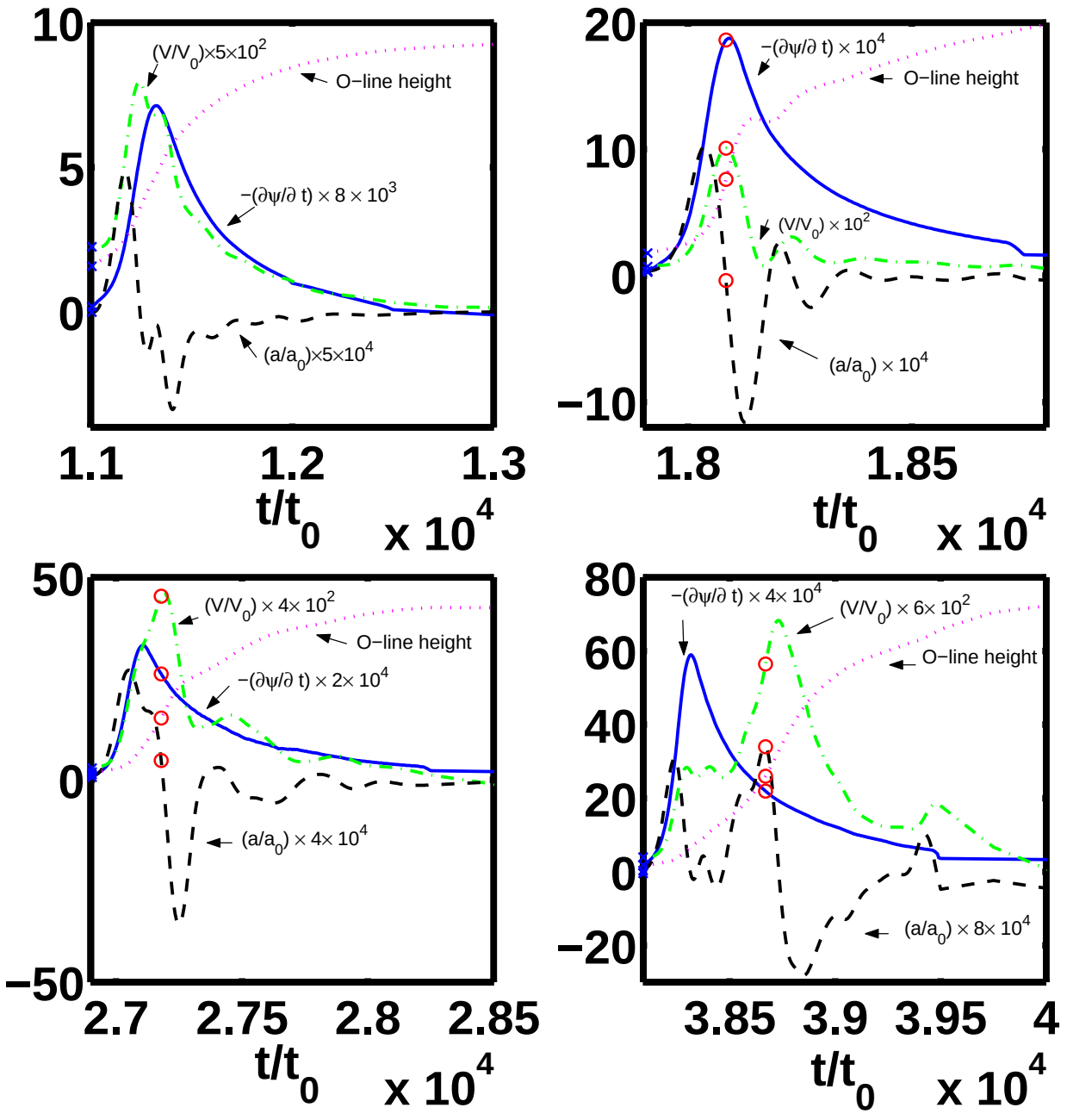

Fig. 4.— The time evolution of the flux rope's O-line height, speed, and acceleration as well as the magnetic reconnection rate in the current sheet for the four reconnection events shown in Fig. 2.

External Distribution

Plasma Research Laboratory, Australian National University, Australia
Professor I.R. Jones, Flinders University, Australia
Professor João Canalle, Instituto de Fisica DEQ/IF - UERJ, Brazil
Mr. Gerson O. Ludwig, Instituto Nacional de Pesquisas, Brazil
Dr. P.H. Sakanaka, Instituto Fisica, Brazil
The Librarian, Culham Laboratory, England
Mrs. S.A. Hutchinson, JET Library, England
Professor M.N. Bussac, Ecole Polytechnique, France
Librarian, Max-Planck-Institut für Plasmaphysik, Germany
Jolan Moldvai, Reports Library, MTA KFKI-ATKI, Hungary
Dr. P. Kaw, Institute for Plasma Research, India
Ms. P.J. Pathak, Librarian, Insitute for Plasma Research, India
Ms. Clelia De Palo, Associazione EURATOM-ENEA, Italy
Dr. G. Grosso, Instituto di Fisica del Plasma, Italy
Librarian, Naka Fusion Research Establishment, JAERI, Japan
Library, Plasma Physics Laboratory, Kyoto University, Japan
Research Information Center, National Institute for Fusion Science, Japan
Dr. O. Mitarai, Kyushu Tokai University, Japan
Dr. Jiangang Li, Institute of Plasma Physics, Chinese Academy of Sciences, People's Republic of China
Professor Yuping Huo, School of Physical Science and Technology, People's Republic of China
Library, Academia Sinica, Institute of Plasma Physics, People's Republic of China
Librarian, Institute of Physics, Chinese Academy of Sciences, People's Republic of China
Dr. S. Mirnov, TRINITI, Troitsk, Russian Federation, Russia
Dr. V.S. Strelkov, Kurchatov Institute, Russian Federation, Russia
Professor Peter Lukac, Katedra Fyziky Plazmy MFF UK, Mlynska dolina F-2, Komenskeho Univerzita, SK-842 15 Bratislava, Slovakia
Dr. G.S. Lee, Korea Basic Science Institute, South Korea
Institute for Plasma Research, University of Maryland, USA
Librarian, Fusion Energy Division, Oak Ridge National Laboratory, USA
Librarian, Institute of Fusion Studies, University of Texas, USA
Librarian, Magnetic Fusion Program, Lawrence Livermore National Laboratory, USA
Library, General Atomics, USA
Plasma Physics Group, Fusion Energy Research Program, University of California at San Diego, USA
Plasma Physics Library, Columbia University, USA
Alkesh Punjabi, Center for Fusion Research and Training, Hampton University, USA
Dr. W.M. Stacey, Fusion Research Center, Georgia Institute of Technology, USA
Dr. John Willis, U.S. Department of Energy, Office of Fusion Energy Sciences, USA
Mr. Paul H. Wright, Indianapolis, Indiana, USA

The Princeton Plasma Physics Laboratory is operated
by Princeton University under contract
with the U.S. Department of Energy.

Information Services
Princeton Plasma Physics Laboratory
P.O. Box 451
Princeton, NJ 08543

Phone: 609-243-2750
Fax: 609-243-2751
e-mail: pppl_info@pppl.gov
Internet Address: http://www.pppl.gov